

Chapter

Synthesis of Polyimides in the Melt of Benzoic Acid

*Kuznetsov Alexander Alexeevich
and Tsegelskaya Anna Yurievna*

Abstract

Review of the authors' works on the synthesis of polyimides (PIs) by the method of one-stage high-temperature polycondensation in an unusual solvent—molten benzoic acid (BA). Compared with a known synthesis in inert high-boiling solvents, synthesis in BA takes place under mild conditions (140°C, 1–2 hour) to give completely imidized PIs. The approach has a number of advantages. Due to catalysis of the first reversible stage of amic acid (AA) formation and low equilibrium constant ($K = 10\text{--}20$ l/mol), the first stage disappears kinetically, and the imidization reaction becomes limiting. The process becomes less sensitive to the basicity of diamines; therefore, low reactivity diamines can be involved. Water is easily removed from the melt by evaporation, which makes the whole process irreversible. Specific features of the method are successfully used to control the microstructure of the chain copolyimides (statistical to multiblock) and to synthesize hyperbranched PIs and star-shaped PIs with narrow molecular weight distribution.

Keywords: Polycondensation, catalysis, benzoic acid, polyimides, block copolymers, hyperbranched polymers, star-shaped polymers

1. Introduction

Aromatic polyimides (PIs) are a class of polymers with a unique combination of properties. Their main advantages are high physical and mechanical characteristics in a wide range from cryogenic temperatures up to 250–300°C and heat resistance up to 400–450°C, etc. Factors that provide such a set of properties of PIs—the presence of conjugated heteroaromatic fragments, strong intermolecular interaction, and chain stiffness—at the same time create difficulties in their processing. Several approaches to the synthesis of PIs are known. The most widespread are the two-stage and one-stage high-temperature methods for the synthesis of PIs from diamines and aromatic tetracarboxylic acids dianhydrides. The general reaction scheme leading to polyimide formation from diamines and dianhydrides consists in two discrete steps: polyacylation to give polyamic acid and imidization (cyclodehydration). The fundamental aspects of the two-stage process of PI synthesis have been the subject of detailed study of many researchers [1–3]. One of the fundamentally important results obtained was the conclusion that the formation of polyamic acids (PAA) is a reversible reaction [4, 5]; the equilibrium constant and degree of polymerization are controlled by the solvent basicity and temperature. This means that to obtain a PAA with a high degree of polymerization, the process is

to be carried out in highly basic (amic) solvents at 20–40°C. In the case of one-stage process in high-boiling solvents, both reactions proceed simultaneously. In the process of one-stage high-temperature polycondensation (HTPC) of diamines and tetracarboxylic acids dianhydrides, the reactions of acylation and cyclization occur simultaneously in a high-boiling solvent at 180–210°C. The synthesis of PIs according to this scheme was first reported by Korshak, Vinogradova, and Vygodskii in 1967 [6–8]: the synthesis of so-called cardo-PIs. This approach has found wide application.

PI synthesis in molten benzoic acid (BA) described in this review should be considered as a variant of the said PI synthesis by HTPC approach. The advantages of using molten BA compared to other high-boiling solvents used in this process (nitrobenzene, m-cresol, o-dichlorobenzene, etc.) are a strong catalytic effect, the lack of solvent toxicity, and easy isolation of polymer due to crystallization of solvent on cooling. In contrast to other novel ecologically improved (“green”) solvents for polyimide synthesis such as ionic liquids [9] and supercritical CO₂ [10], this approach does not require any special chemicals and equipment.

2. General features of the process

2.1 Rate of the process and molecular weight

The process of synthesis of PIs in molten BA can be carried out under relatively mild conditions (140°C, 1–2 hour) at slow inert gas flow [11–13]. Within 1 hour after the start of synthesis, fully cyclized polyetherimides (PEIs) and PIs with logarithmic viscosity values $\eta_{\log} = 0.4\text{--}1.2 \text{ dL}^* \text{g}^{-1}$ (N-methyl-2-pyrrolidone (N-MP), 25°C), depending on the structure of the monomers, were isolated. In the IR spectrum of the products, there are typical absorption bands of the imide cycle in the regions of 720, 1370, 1720, and 1780 cm^{-1} ; no peaks of amic acid fragments (1660 cm^{-1} , 3600 cm^{-1}) were observed. Imide peaks in IR spectrum did not change after additional heat treatment of polymers at 300°C for 0.5 hour; this allows us to conclude that during the synthesis, almost 100% conversion of imidization has been achieved. Molecular weight $M_w = 5\text{--}15 \cdot 10^4$ (GPC) is sufficient for the subsequent processing of PIs into films, semifinished products, and bulk products by extrusion and injection molding or for use as binders for composite materials. The rate of PEI molecular weight increase, when synthesized in the BA melt at 140°C, is significantly higher than that in m-cresol at the same temperature.

The ability of carboxylic acids as additives to accelerate the process of one-pot synthesis of PIs was first demonstrated for synthesis of PIs with cardo fragments in nitrobenzene [14] at 160–210°C. However, it was noted that with an increase in the concentration of BA in a system above 2.5 mol BA per 1 mole of repeating unit (about 10%-weight solution in reaction mixture), the total rate of the process decreases—up to complete inhibition—probably due to the fact that the excess BA deactivates the amino group by the mechanism of acid–base interaction. In our works, we used concentration up to 95% in reaction mixture BA as a solvent. Under these conditions, the (BA/repeating unit) mole ratio is about 30–35. The absence of inhibition by excess BA can be explained by the fact that the melt of BA is a nonpolar liquid—by analogy with 100% acetic acid (AcOH) which has dielectric constant $k \sim 6$; therefore, the dissociation constant BA in its own melt can be significantly lower than that in nitrobenzene.

The general scheme of the process of obtaining PIs by high-temperature polycondensation of diamines and dianhydrides can be represented as follows (**Figure 1**). **Figure 1** includes four conjugated reactions, including two main ones, acylation and

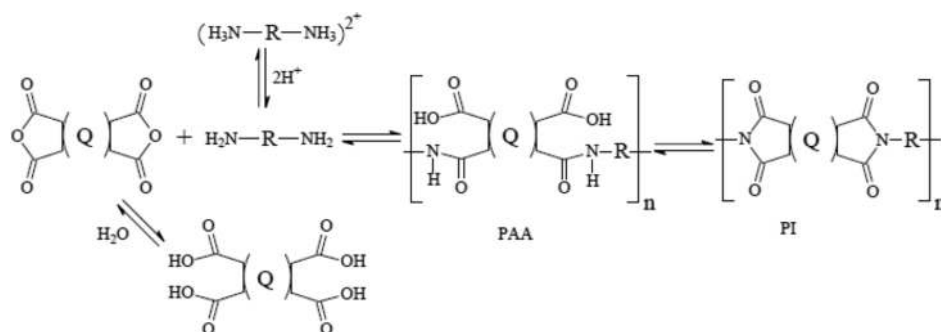


Figure 1.
 Scheme of PIs obtaining by polycondensation of diamines and dianhydrides.

imidization, and two side reactions, binding of amino groups by acidic medium and hydrolysis of anhydride groups by water released during imidization. The degree of reversibility of each reaction depends on the temperature, acidity of solvent, and rate of water vapor removal. The replacement of dianhydride for corresponding tetracarboxylic acid does not influence on the overall rate and final molecular weight. This allows suggestion that dehydratation of diphtalic acids is reversible and fast.

2.2 Leveling of monomer reactivity

In the course of experiments with different monomer pairs (**Table 1**), it was found that the chain growth rate in molten BA showed a rather weak dependence on the basicity of the diamines used [13, 15, 16]. This observation is in stark contrast to regularities of the low-temperature polycondensation in amic solvents in which the basicity of the diamines has a strong influence on the rate of polycondensation [1–3]. Such phenomenon of partial “reactivity leveling” in molten BA is of interest as a method of obtaining new high molecular weight copolyimides from low reactive diamines. In **Table 2**, the logarithmic viscosity (η_{\log}) values are given of polyimides synthesized in molten BA from dianhydrides and bridged aromatic diamines having different basicities expressed as pK_b values.

It was observed that the change in basicity index of aromatic diamines in a range from $pK_b = 5.5$ (ODA) to $pK_b = 2.5$ (SDA) did not result in a significant difference in η_{\log} of final PIs (**Table 2**). It allows a conclusion that conversion of amino groups reached for 1.5 h was at least 90–95% in both cases. In other words, the difference in apparent reactivity of diamines of both the low and the high basicities is not so large. Such a behavior is quite different from the results reported for low-temperature polycondensation of diamines and dianhydrides in amide solvents. For the latter reaction, changing the type of bridge substituent in diamines in a row —O—; —CH₂—; —SO₂— results in about three orders of magnitude decrease in the rate constant of polycondensation with pyromellitic dianhydride [1–3].

2.3 Mechanism and kinetics

Initially, we suggested that low sensitivity of reaction rate to basicity of diamines is caused by interaction with acid medium, i.e., the higher the basicity of amino group, the higher its deactivation by acid medium. To check this supposition, we studied a character of interaction of different diamines with BA by the method of the phase diagrams.

In **Figure 2a, b**, the phase diagrams are shown of binary system BA-diamine constructed on the basis of DSC thermograms for BA-diamine mixtures of different compositions [15]. It is seen that highly basic 1,12-dodecamethylene diamine with

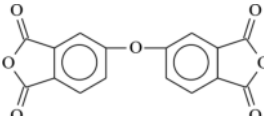
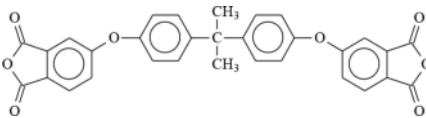
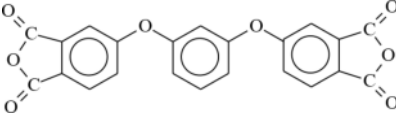
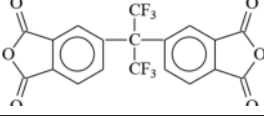
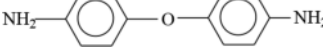
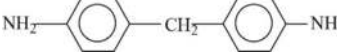
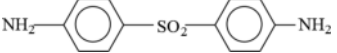
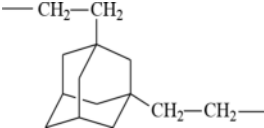
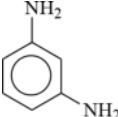
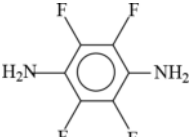
	ODPA	Oxydiphthalic dianhydride
	BPADA	Dianhydride of 2,2-bis-[(3,4-dicarboxyphenoxy)phenyl]propane
	RDA	1,3-Phenylenedioxy-bis-4-phthalic anhydride
	6F	2,2-Hexafluoropropylidene-diphthalic anhydride
	ODA	4,4'-Oxydianiline
	MDA	4,4'-Methylenedianiline
	SDA	4,4'-Sulfonyldianiline
$\text{H}_2\text{N}-(\text{CH}_2)_6-\text{NH}_2$	HMDA	1,6-Hexamethylenediamine
$\text{H}_2\text{N}-(\text{CH}_2)_{12}-\text{NH}_2$	DDA	1,12-Dodecamethylene diamine
	ADA	1,3-Bis-(2-aminoethyl)-adamantane
	m-PDA	m-Phenylene diamine
	TFPDA	Tetrafluoro-p-phenylene diamine

Table 1.
Monomers used for polycondensation.

Diamine	Dianhydride	$\eta_{\text{log}}(\text{dL g}^{-1})^a$
ODA ($\text{pK}_b = 5.5$)	ODPA	0.57 (H_2SO_4)
SDA ($\text{pK}_b = 2.5$)	ODPA	0.44 (N-MP)
ODA	BPADA	1.0 (N-MP)
SDA	BPADA	0.45 (N-MP)

^aN-MP, 0.5 g/dL, 25° C

Table 2.
Characterization of polyimides obtained in molten BA, at 140° C (1.5 hour) [12].

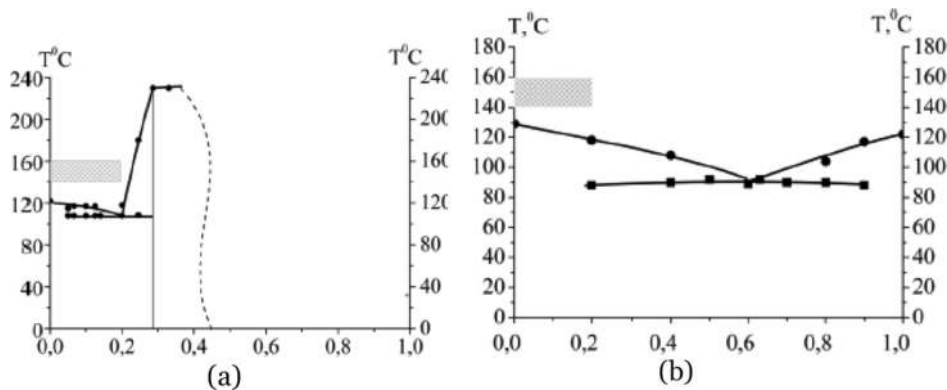


Figure 2. Phase diagrams of binary system BA-diamines: DDA (a) and ODA (b); point (0.0) corresponds to 100%-Mol BA and point (1.0) to 100%-Mol diamine [15].

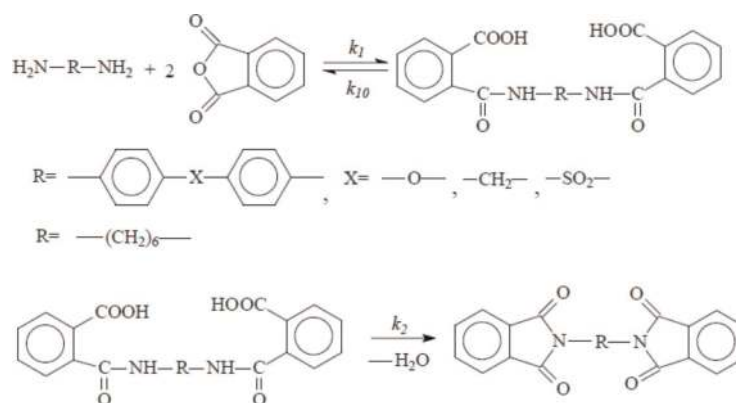


Figure 3. Model reactions of amic acid formation and imidization.

low melting point ($T_m = 67^\circ\text{C}$) interacts with BA to form alkyne-bis-ammonium benzoate (**Figure 2a**) with $T_m = 236^\circ\text{C}$, whereas less basic ODA does not form such a salt; the phase diagram of BA-ODA system has an appearance of ordinary physical mixtures of two substances with limited solubility in each other (**Figure 2b**).

We also investigated the kinetics of model reaction—acylation of diamines ODA, MDA, SDA, and HMDA by phthalic anhydride (PhA) in glacial AcOH (**Figure 3**).

Kinetic data were obtained by potentiometric titration of amino groups with solution of perchloric acid in AcOH after reaching an equilibrium state [16, 17]. Results are presented in **Table 3** [16, 17]. It is seen that at the initial period of acylation, kinetics obeys the equation of second-order reaction (**Figure 4**); considerable difference is observed in the rate constants of bridged

Diamine	k_1 (mole * min) ⁻¹ (22°C)	K_p (mole) ⁻¹ (22°C)	E_a (kJ*mole ⁻¹)	$-\Delta H$ (kJ* mole ⁻¹)
ODA	490	8670	34.4	44.0
MDA	175	5800	33.1	41.5
SDA	6.9	1130	28.1	40.6
HMDA	0.054 ^a	95.6 ^a	77.1	13.0

^aExtrapolated value.

Table 3. Parameters of the acylation reaction of different diamines in glacial acetic acid.

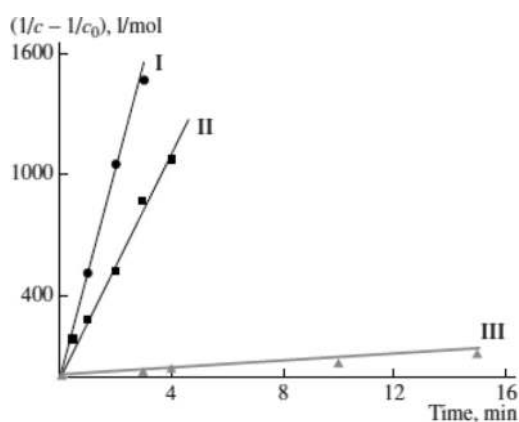


Figure 4. Acylation kinetics of diamines ODA (I), MDA (II), and SDA (III) with phthalic anhydride in AcOH at 22°C (second-order reaction plot). Starting concentration of amino groups: ODA, 0.005; MDA, 0.01; and SDA, 0.03 Mol L⁻¹ [16].

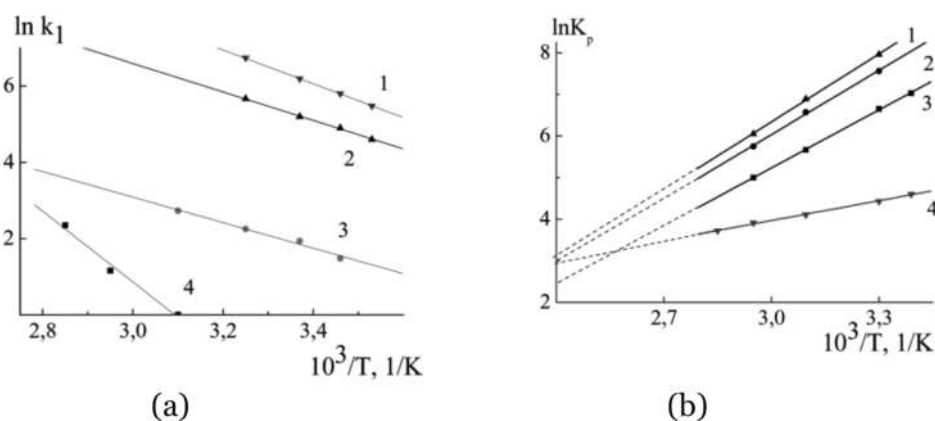


Figure 5. Arrhenius plots (a) and logarithm of the equilibrium constant vs. the reciprocal temperature (b) for the acylation of diamines ODA (1), MDA (2), SDA (3), and HMDA (4) with phthalic anhydride [16, 17].

—O—; —CH₂—; —SO₂— diamines. So, partial effective reactivity leveling in a row of aromatic diamines (not able to form salt) observed experimentally in one-pot PI synthesis in molten BA at 140°C hardly can be explained by difference in acid–base-type interaction of amino groups with BA.

Alternative explanation of this phenomenon is the change of limiting stage from amic acid moiety formation for amic acid moiety imidization; the latter is much less sensitive to chemical structure of starting reagent.

From Arrhenius plots (**Figure 5a**), the values of activation energy (E_a) of acylation in glacial acetic acid (AcOH) were determined (**Table 3**). At elevated temperatures (50°C and higher), the reversible character of the acylation was established. On the basis of experimentally measured equilibrium amino group concentration, the equilibrium constants (K_p) were determined at different temperatures. In **Figure 5b**, temperature dependences of equilibrium constants for acylation reaction different diamines with PhA are shown.

From these data, using the vant' Hoff equation, the enthalpy change (ΔH) values for the acylation reaction of diamines in AcOH were determined (**Table 2**). On the basis of the values of the equilibrium constants and the rate constants for direct reaction (k_1), the first-order rate constants for the back-reaction (k_{-1}) were calculated for each temperature. In **Table 4**, the values of rate constants at 140°C obtained by extrapolation are given.

Diamine	k_1 (l*mole ⁻¹ min ⁻¹) ^a	k_{-1} (min ⁻¹) ^a	K_p (l*mole ⁻¹) ^a	k_2 (min ⁻¹) ^b
ODA	24,200	960	25.2	0.8
MDA	8100	370	22.0	—
SDA	150	15.6	9.6	0.4
HMDA	430	20	21.4	0.6

^aExtrapolated.

^bExperiment in closed system.

Table 4.
Parameters of acylation and imidization in carboxylic acid media (140°C).

It should be noted that a very low acylation rate was observed in the case of aliphatic diamines at 22°C (**Table 3**). The reason is occurrence of the concurrent reaction of salt formation with AcOH. This conclusion is confirmed by the appearance of adsorption peaks of benzoate anion and alkylene-bis-ammonium cation in IR spectrum.

Formation results in increase in effective activation energy of acylation. Due to this, the acylation rate increases sharply with increasing temperature (**Figure 5a**, line 4, and **Tables 3 and 4**).

We also estimated the value of effective rate constants for the imidization step [16, 17]. Low molecular weight model amic acids were synthesized from ODA, SDA, and HMDA and PhA. Kinetics of their imidization in the melt of BA at 140°C was followed by FTIR. First-order reaction rate constants were determined and corrected taking into account the conjugated reactions of decay and resynthesis of amic acid. Corresponding set of kinetic equations was written and solved numerically to give best fitting with experimental data on kinetics of imide cycle accumulation. From the analysis of the kinetic data, the following conclusions are apparent:

1. Imidization of amic acid moieties at 140°C in molten BA acid medium is a first-order reaction with a very fast pre-equilibrium stage (**Figure 3**).
2. Due to catalysis of the acylation step in molten BA in combination with low equilibrium constant, this stage becomes kinetically insignificant, and imidization becomes the rate-determining step of PI formation. In comparison with acylation reaction, imidization is less sensitive for chemical structure of reagents, so in one-pot PI synthesis, partial effective reactivity leveling of the low and high reactive diamines is observed.

3. Synthesis of random and multiblock copolymers

Multiblock (MB) copolymers attract big attention due to their ability to self-organize and form continuous two-phase morphology with controlled characteristic size of the phase particle in the micro- or nanoscale range. MB copolyimides (MB CPIs) are also known as promising materials for design of gas separation and proton-conductive membranes for fuel cells.

Conventionally, polycondensation-type MB copolymers are synthesized by polycondensation of two preliminary synthesized oligomers containing terminal reactive groups. MB CPIs can also be obtained by transimidization reaction of oligoimides with pyrimidine end groups. The limitation of this approach is the fact that only few oligoimides are soluble in organic solvents.

Vasnev and Kuchanov [18] investigated theoretically the regularities of copolymer chain microstructure formation in the course of copolycondensation in a system ($A_2 + B_2 + C_2$). Here A_2 and B_2 are the same type bifunctional monomers of different reactivities; C_2 is bifunctional “intermonomer” which reacts with A_2 and B_2 ; monomer A_2 does not react to B_2 . According to this theory, MB copolymer can be formed from the system ($A_2 + B_2 + C_2$) in a regime of slow loading of intermonomer C_2 to the mixture of comonomers $A_2 + B_2$, but only in the case if polycondensation process meets the following requirements (so-called “ideal” interbipolycondensation): (1) reaction is irreversible; (2) any difference in reactivity of A_2 and B_2 occurs; any by-reactions are absent; and (3) reaction system is homogenous.

We synthesized a series of CPI samples from BPADA (intermonomer) and different pairs of diamines (CPI-1 series, **Figure 6**) in the melt of BA at 140°C with variable order of intermonomer loading [19]. In [20], two more CPI series (CPI-2 and CPI-3) were synthesized using dianhydrides OPA and RDA as intermonomer and AFL and DDA as comonomers (**Figure 7**). Starting comonomers in all cases were chosen taking into account the solubility of copolymers in $CDCl_3$.

Chain microstructure of CPIs was studied by high-resolution NMR ^{13}C . In **Figure 8**, selected “sensitive” regions of NMR ^{13}C spectra (134–136 and 161–162 ppm) are shown for samples prepared of CPI-2 series. Designation *aa*, *bb*, and *ab* renders to monomer moiety consequences in chain: ACA, BCB, and ACB, correspondingly.

In **Figure 8**, curves 3–5 the inner two signals in 134–135 and 160–161 ppm regions correspond to *aa* and *bb* triads, and the outer two corresponds to *ab* triads. In the 113–114-ppm region, only one *ab* signal is observed. Analogous signal attribution was executed for every other CPI samples. Distribution of comonomer moieties in copolymer chain was characterized quantitatively by the coefficient of chain microheterogeneity (K_m ; Eq. (1)) introduced by Yamadera and Murano [21]:

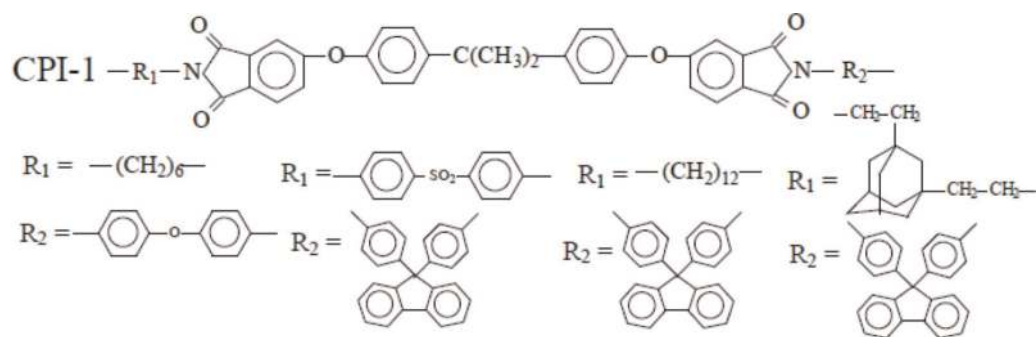


Figure 6.
Chain structure of copolyimides of CPI-1 series.

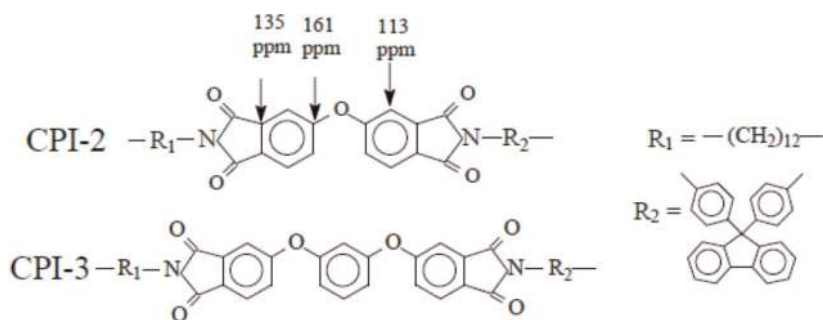


Figure 7.
Chain structure of copolyimides of CPI-2 and CPI-3 series.

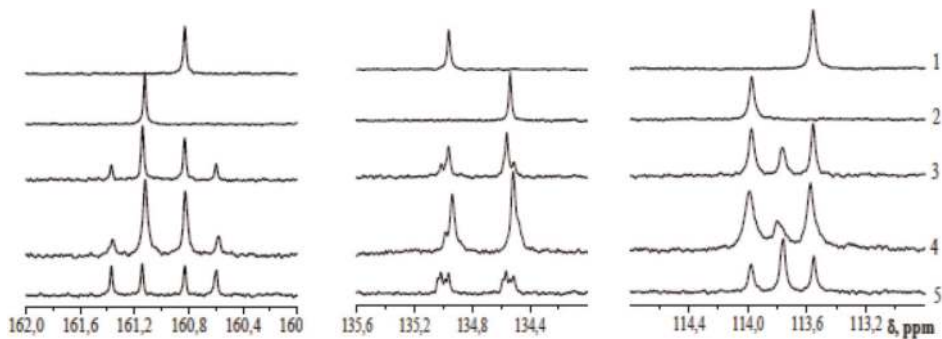


Figure 8. NMR ^{13}C spectra of CPI-2 series and corresponding homopolyimides in the structure-sensitive regions. Numbers to the right of curves correspond to the experiment number in **Table 5**. Signal attribution to the *aa*, *bb*, and *ab* triads was executed by comparison with signals of homopolyimides (**Table 6**).

Experiment	Sample (order of loading, mole parts)	Triad ratio <i>aa/ab/bb</i>	K_m
1	Homopolyimide DDA-ODPA	1/0/0/	—
2	Homopolyimide AFL-ODPA	0/0/1	—
3	Slow (30 min) addition of ODPA to the mixture DDA/AFL (0.5/0.5)	1.7/1/1.6	0.48
4	Slow (30 min) addition of the mixture ODPA/DDA (1.0/0.5) to AFL (0.5)	2/1/1/1.9	0.39
5	One-shot loading of DDA/AFL/ODPA (0.5/0.5/1.0)	0.55/1/0.62	0.92

Table 5. Loading condition and characteristics of CPI-2.

$$K_m = \frac{P_{ab}}{P_{ab} + 2P_{aa}} + \frac{P_{ab}}{P_{ab} + 2P_{bb}} \quad (1)$$

where P_{aa} , P_{bb} , and P_{ab} are the fractions of corresponding *aa*, *bb*, and *ab* triads.

The average block length l_A , l_B can be calculated as a unit divided by the first and second term in Eq. (1), correspondingly. In such a description, values $K_m = 0$; l_A , $l_B = \infty$ correspond to the mixture of two homopolymers; $K_m = 1$; l_A , $l_B = 2$, for random copolymer, and $K_m = 2$; l_A , $l_B = 1$, for strict alternation of moieties in copolymer. K_m values calculated from experimental NMR ^{13}C data for the samples of CPI-1–3 are shown in **Table 5**.

As it is seen from **Table 5**, at slow addition of intermonomer, in all experiments, we have obtained block CPIs with five-membered imide cycles. In the case of simultaneous loading, only random CPI was obtained. These results differ from data obtained in a work [22], in which only random CPI with five-membered imide cycles was obtained when conventional high-boiling solvent was used at any character of intermonomer addition to the mixture of diamines.

In **Figure 9**, NMR ^{13}C spectra are given for sample CPI-4 series, in which 1,3-bis(2-aminoethyl)adamantane (ADA) was used as intermonomer, and two anhydrides of different reactivities—BPADA and 6F (**Table 1**)—as comonomers (**Figure 10**) [23]. Curves 1 and 2 refer to homopolymers; curves 3 and 4 to the CPI-4 samples, obtained with simultaneously monomers loading and slow intermonomer loading, correspondingly. Attribution to triads is the following (ppm): 46.51 (*aa*), 46.63 (*ab*), and 46.71 (*bb*). The values of K_m and average block length calculated from the NMR ^{13}C spectra are $K_m = 0.91$ (l_A , $l_B = 2.2$) for simultaneous comonomer loading and $K_m = 0.76$ (l_A , $l_B = 2.63$) for slow loading of intermonomer. This result is

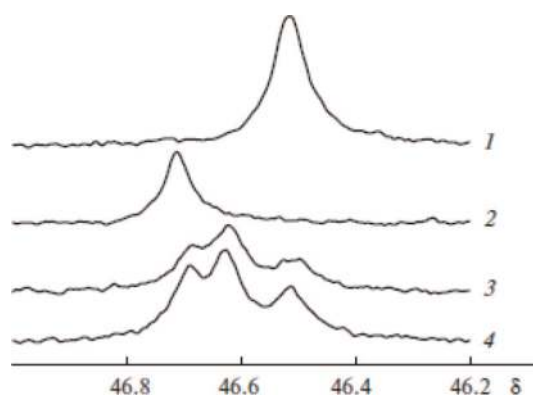


Figure 9.
A structure-sensitive region of the NMR¹³C spectra of CPI-4 series.

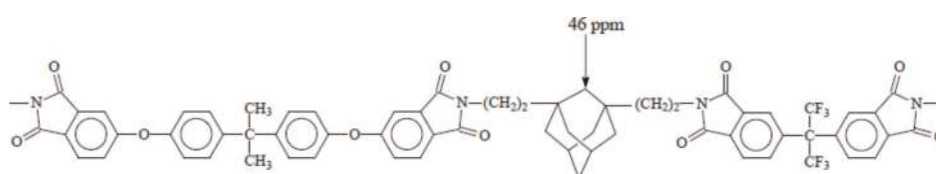


Figure 10.
Chain structure of copolyimides of CPI-4.

indicative of trend of formation of a multiblock chain microstructure at slow intermonomer loading.

This trend is not very pronounced in the comonomers chosen and shows rather weak influence of chemical structure of anhydride component on reactivity in molten BA.

In [24, 25], mathematical model has been developed by us for chain microstructure formation in copolyimide (CPI) synthesis (CPI) from two diamines A and B (comonomers) and one dianhydride C (intermonomer) in molten BA different regimes of intermonomer loading. The kinetic scheme was analyzed involving acylation of both diamines with anhydride fragment, decomposition, and imidization of two intermediate amic acid fragments.

Kinetic constants of acylation and imidization stages necessary for calculations were taken from our earlier experiments with model reactions described in Part 2.3 of this review. By numerical solution of the system of kinetic equations for different regimes of intermonomer loading, we calculated dependences of the change in time of the average block length l_A , l_B , the current concentrations of amino and anhydride groups, amic acid fragments, imide cycles, and triads aa , bb , and ab for CPI-1–3. The calculated values of the average block length and the chain microheterogeneity parameter ($K_m = 0.5$ – 0.6) for several comonomer pairs at slow intermonomer loading are in good agreement with the experimental values obtained from NMR ¹³C data.

The kinetics of the block length (l_A and l_B) growth for regime of the slow intermonomer loading (for 30 min) is given in **Figure 11**. The length of block (l_A) containing the moieties of more active comonomer reaches its final value $l_A = 4$ already to the end of intermonomer loading, whereas the block length l_B goes on to increase. In the end, block copolymer forms. The difference in times of block formation is the sequence of difference in comonomer reactivity.

Typical consumption kinetics of amino and anhydride groups is presented in **Figure 12**. Consumption rates of amino groups belonging to the first and the second comonomers differ considerably. Concentration of transient amic acid fragments is

<i>aa</i>	<i>ab</i>	<i>bb</i>
160.82	160.60; 161.37	161.12
134.96	135.01; 134.51	134.53
113.56	113.77	113.97

Table 6.
 Attribution of signals in NMR¹³C spectra of CPI-1 series to triads.

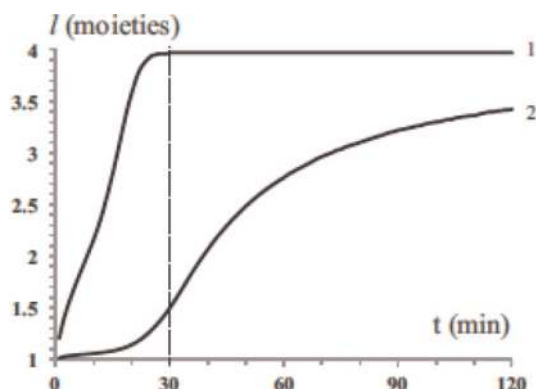


Figure 11.
 Typical curve of change in time of the average length of blocks l_A (1) and l_B (2) in experiment with slow loading of the intermonomer (30 min).

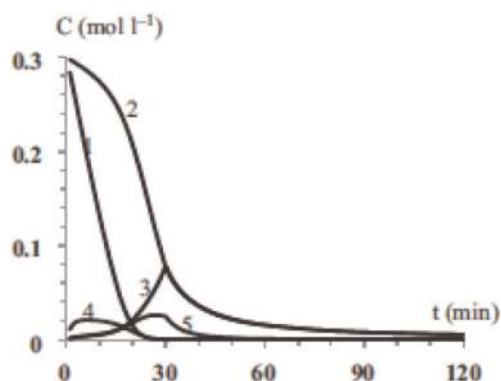


Figure 12.
 Typical curves of change in time of the concentration of amino groups of A (1) and B (2), anhydride groups C (3), and amic acid fragments (4, 5).

low, less than 10% of starting amino groups. These fragments react rapidly to give imide cycles.

Kinetics of accumulation of imide cycles and different types of triads (*aa*, *bb*, and *ab*) are presented in **Figure 13**.

Accumulation of imide cycles and *aa* triads from the more reactive comonomer occurs faster than that for the less reactive monomer and forms a block consisting of several triads *aa*. Concentration of imide cycles and triads *bb* from less reactive comonomer increases with conversion more slowly. So, the model developed by us can be used to predict microstructure of the CPI chains at any conversion and at any loading order of intermonomer and comonomers. Dependence of parameter K_m for the final CPI on the duration of intermonomer BPADA loading for system AFL-DDA is presented in **Figure 14**. It should be noted that the fact of influence of intermonomer loading order on chain microstructure is very important for

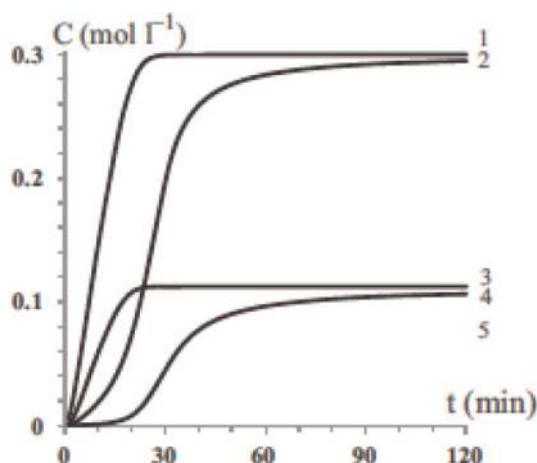


Figure 13.

Typical curves of change in time of the concentration of imide cycles (1,2) and triads: aa (3), bb (4), ab (5).

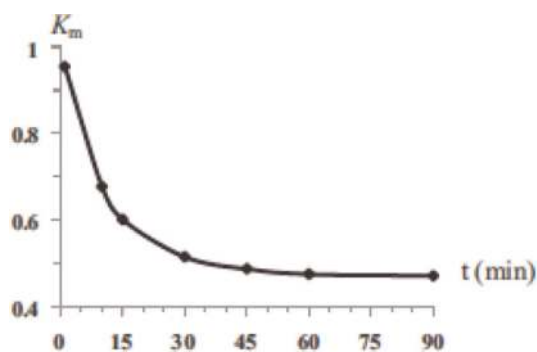


Figure 14.

Dependence of parameter K_m for CPI (120 min) on duration of intermonomer loading.

understanding the mechanism of PI synthesis in molten BA. The process shows symptoms typical for ideal interbipolycondensation. This means that the basic reaction—imidization—is practically irreversible at these conditions, i.e., the rate of evacuation with inert gas flow of the vapor of water released in the course of imidization is high. Otherwise, formation of long blocks would be impossible.

4. Synthesis of (hyper)branched (HB) polyimides

Investigation of hyperbranched (HB) polymers is a new rapidly developing field of polymer chemistry. HB polyimides (HB PIs) are of special interest for development of new functional materials as they can combine unique characteristic properties of polyimides (thermal and chemical stability, photostability barrier properties, etc.) with some common characteristic properties of HB polymers (solubility, possibility of placing many functional groups in one macromolecule, etc.). Examples are described in applying HB PI as proton-conductive or gas separation membranes, photosensible materials, etc. The study of these objects is largely constrained by multistage synthesis and a number of difficulties encountered in the synthesis process. Therefore, the creation of a simple convenient synthesis methodology is an important task.

In our work [26], we used the method of one-pot high-temperature polycondensation in molten BA at 140°C for synthesis of HB PIs with reactive anhydride

groups via scheme $A_3 + B_2$, the monomer B_2 being AFL, and monomer A_3 —trianhydride of hexacarboxylic acid prepared by reaction of 1,3,5-triaminotoluene sulfate with excess of BPADA. The A_3/B_2 ratio was chosen 1:1-mol. HB PI prepared was found to have wide MWD, and the glass temperature was $T_g = 235^\circ\text{C}$, which is 55°C less than that for corresponding linear PI AFL-BPADA. In a frame of $A_2 + B_3$ approach, HB PI with terminal amino groups was prepared from 2,4,6-tris-(4-aminophenoxy)toluene and BPADA [27]. New HB polyimide with terminal amino groups was prepared also in molten BA via $A_2 + B_4$ scheme by polycondensation of 1,4-bis(3,5-diaminophenoxy) benzene (BDAPB, B_4) dialkyl semi-ester derivative of BPADA (precursor of A_2) obtained by treatment of BPADA with boiling ethyl alcohol (Figure 15) [28]. Structure of the products was confirmed by IR and NMR spectroscopy.

IR spectrum of synthesized HB PI sample (Figure 16a, curve 2) contains characteristic absorption bands at 1720 and 1780 cm^{-1} (antisymmetric and symmetric stretch $\text{C}=\text{O}$ vibrations of imide cycle). The absorption band retains at $3300\text{--}3050\text{ cm}^{-1}$ which is observed also in the spectrum of starting B_4 (stretch N-H vibrations of amino groups) (Figure 16a, spectrum 1).

The final polymer product was obtained as beige color powder soluble in THF, DMSO, and amic solvents. Mw of HB PI obtained is of about $2 \cdot 10^4$. In NMR ^1H

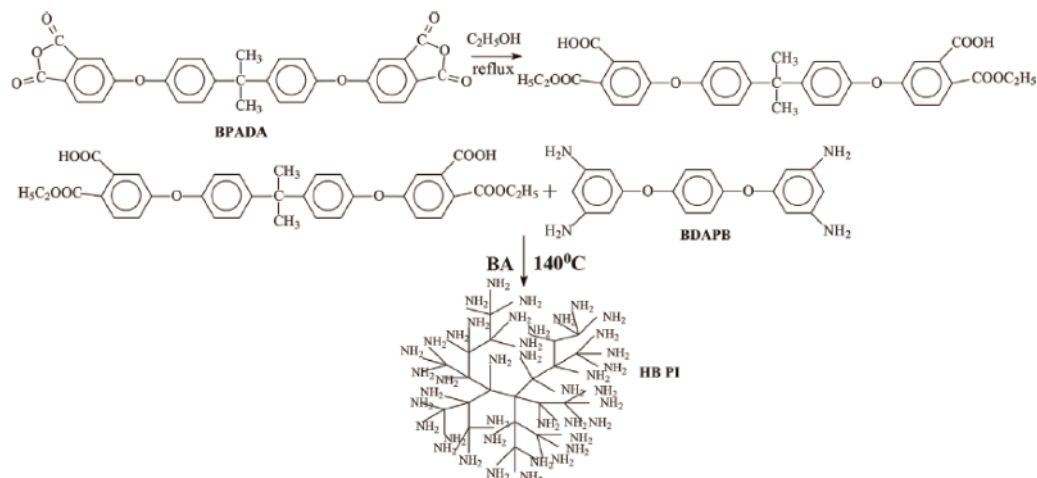


Figure 15.
Synthesis of hyperbranched polyimide.

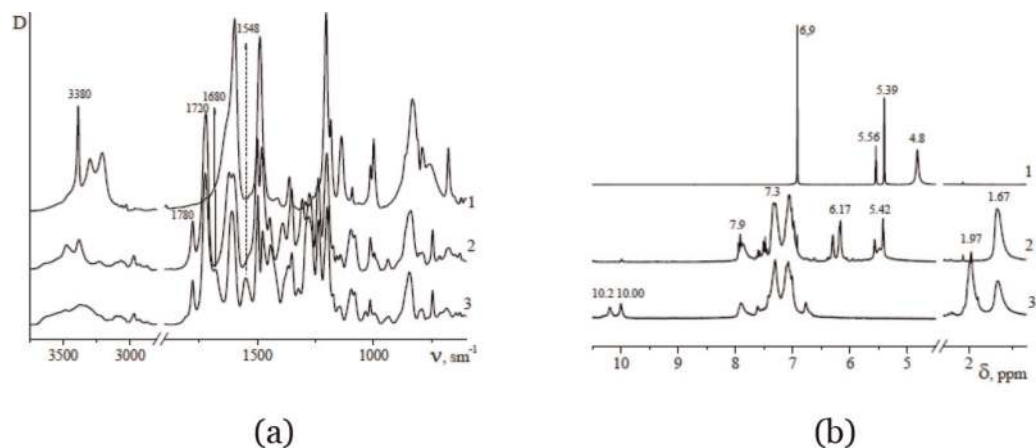


Figure 16.
Review IR spectra (a) and NMR ^1H spectra (b) of monomer B_4 (1), HB PI (2), and HB PIac (3).

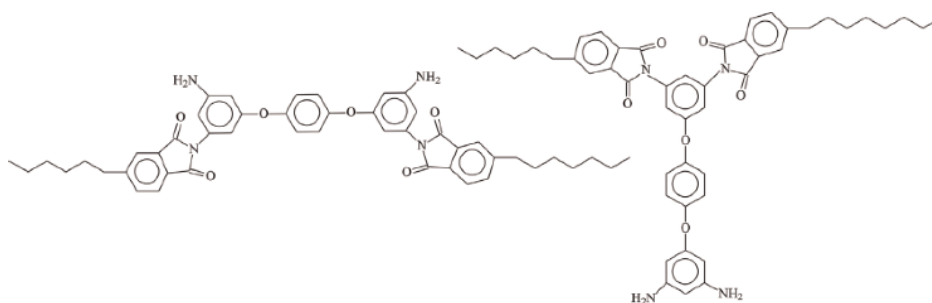


Figure 17.
Isomeric “linear” fragments in hyperbranched polyimide.

spectra of the starting B4 monomer (**Figure 16a**, spectrum 1), there are signals of protons of amino groups at 4.8 ppm, two signals of protons of aromatic fragments nearest to amino group at 5.58 and 5.42, and one signal of protons of central aromatic cycle at 6.9 ppm. In a spectrum of HB PI (**Figure 16b**, spectra 2), the signals of amino groups are shifted to 5.4 and 5.8 ppm due to appearance of imide fragments. Also, new signals of aromatic protons appear at 7–8 ppm belonging to protons of aromatic nuclei of dianhydride fragment as well as signals of isopropylidene fragment at 1.67 ppm.

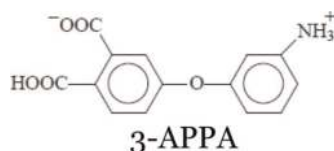
With the presence of reactive terminal amino groups in HB PI, we carried out its reaction with acetic or phthalic anhydrides (at 25°C in dimethylacetamide and in molten BA, respectively). In IR spectra of the product isolated after treatment with acetic anhydride (HB PIac) (**Figure 16a**, curve 3), an absorption band at 3300–3500 cm^{-1} (NH_2 group) disappears, and new bands at 1680 and 1550 cm^{-1} (deformation N-C vibrations, “amide 1” and “amide 2”) appear.

In NMR ^1H spectrum of HB PIac (**Figure 16b**, spectra 3), the signals at 5.4 and 5.8 ppm (NH_2) disappear, and new signals at 10.0 and 10.2 ppm appear related to two isomeric “linear” fragments of HB PIac (**Figure 17**). From the fact of equal intensity of these signals, it should be concluded that reactivity of all amino groups is about the same.

This observation is of importance because on its basis it can be concluded that all four amino groups of B4 monomer participate in chain growth with nearly the same probability, i.e., the scheme of reaction indeed is $\text{A}_2 + \text{B}_4$ and must result in HB polymer.

5. Synthesis of polyimides from “AB” monomers

The one-pot high-temperature catalytic polycyclocondensation in molten BA was successfully used to obtain homo- and co-PEIs from 4-(3-aminophenoxy)-phthalic acid (3-APPA) which has a structure of latent “AB” monomer [29]. In solid state, 3-APPA exists in a zwitterionic form. In molten BA at 140°C, it transfers to the “open” form which is able to dehydrate to give monomer with amino and anhydride groups. It is able for auto-polycondensation with moderate rate. Homo-PEI prepared from 3-APPA in molten BA is high molecular weight amorphous thermoplastic PEI with a glass temperature of 210–220°C soluble in chloroform and DMSO. The yield and degree of imidization are close to 100%. In contrast, homo-PEI prepared at the same conditions from isomeric 4-(4-aminophenoxy) phthalic acid (4-APPA) is insoluble and intractable till 400°C. Properties of copolyimides 3-APPA/4-APPA depend on composition. When the 3-APPA/4-APPA ratio in starting monomer mixture is 30:70 or less, the polymer is amorphous and soluble in organic solvents. At 3-APPA/4-APPA ratios of 40:60 or higher, CPIs lose solubility and tractability.



6. Synthesis of star-shaped polyimides with narrow molecular weight distribution

Star-shaped polymers (SSP) are of special interest among a variety of branching polymers. The state of the art in a field of SSP is considered in several excellent reviews [30]. In many papers, SSP with narrow MWR was synthesized using the methods of controlled chain polymerization. Yokozawa et al. [31] were the first to show that the “step growth” processes also can be applied to obtain SSP with narrow MWD. They synthesized SSP using polycondensation by the scheme ($B_n + AB$), where B_n is a multifunctional core initiator and AB is a low reactive monomer with two different functional groups A and B.

Narrow MWD can be achieved by using special AB' monomers, which are not able for auto-polycondensation, but able to react to active B groups of B_n core initiator. When AB' moiety attaches to B_n , terminal B' group becomes much more reactive due to the changing mesomeric effect in the course of condensation, and selective arm growth occurs.

To synthesize star-shaped oligoimides (SOI), we have used known general reaction scheme $B_3(B_4) + AB$, but another principle providing selective star arm growth not requiring special monomers AB [32, 33]. 1,3,5-(4-Aminophenoxy)toluene (TAPT) was used as B_3 , bis(3,5-diaminophenoxy)benzene (BAPB) as B_4 , and 3-APPA as latent AB monomer.

In the course of synthesis, APPA was introduced slowly to the reaction mixture containing TAPT and BAPB, providing that the current AB concentration in molten BA always being much less than that of TAPT or BAPB. The reaction scheme is given below (**Figure 18**). To check the possibility of obtaining stars with different average arm lengths, the overall 3-APPA/TAPT ratio was varied in a row: 10:1, 20:1, 40:1, and 100:1.

In IR spectra of SOI samples, characteristic absorption bands appear at imide cycle at 1720 and 1780 cm^{-1} (symmetric and asymmetric C=O vibrations). With increase in 3-APPA/TAPT ratio, the intensity of N-H vibrations in NMR ^1H of the model compound obtained by treatment TAPT with excess of phthalic anhydride (TAPT-PhA) of terminal NH_2 group at 3380–3480 cm^{-1} decreases.

Comparison of the NMR ^1H spectra of TAPT (**Figure 19**) and the model compound TAPT-PhA, obtained by treatment of TAPT with phthalic anhydride (PhA) (**Figure 19**), shows that the replacement of the amino group on phthalimide group results in disappearance of the signal of the amino group protons (5.0 ppm) and the signal shift (from 5.8 to 6.6 ppm) of c, d, e, and f protons (**Figure 20**) belonging to central aromatic ring. There are new signals in the region of 8.0 ppm, referred to the protons “u, z” of the phthalimide fragment. Similar changes are observed in the spectra of SOI: c, d, e, and f signals are shifted downfield. From the comparison of NMR spectra of SOI 10 and SOI 40 (**Figure 19**), it is seen that the intensity of proton signals of terminal amino groups “p” at 5.4 ppm and methyl group of the central fragment (2.08 ppm) decreases with an increase in the APPA/TAPT ratio. Weak signals at 6.2–6.5 ppm are referred to aromatic protons “k, l, n” of the terminal fragment containing amino group. The structure of SOI is confirmed by the results of integration of NMR ^1H signals.

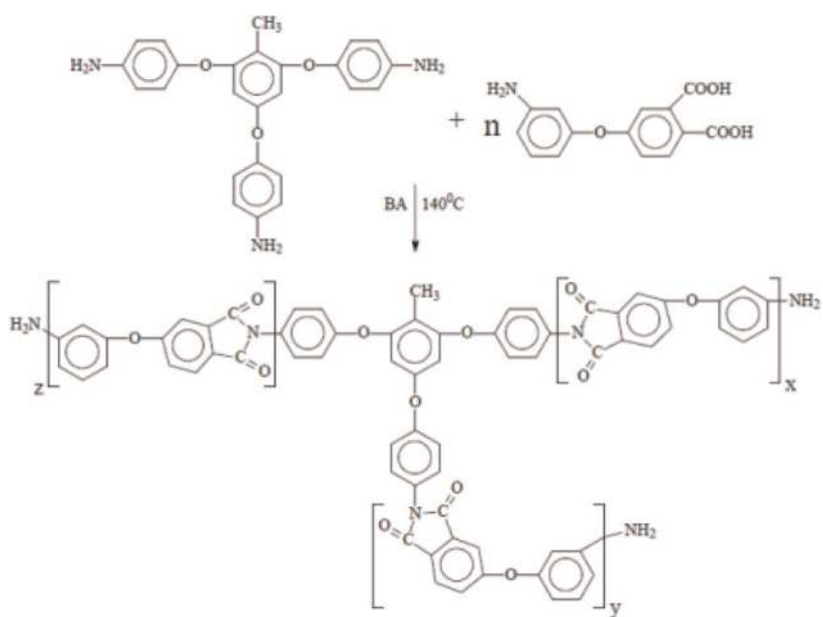


Figure 18.
Synthesis of 3-arm star-shaped polyimide.

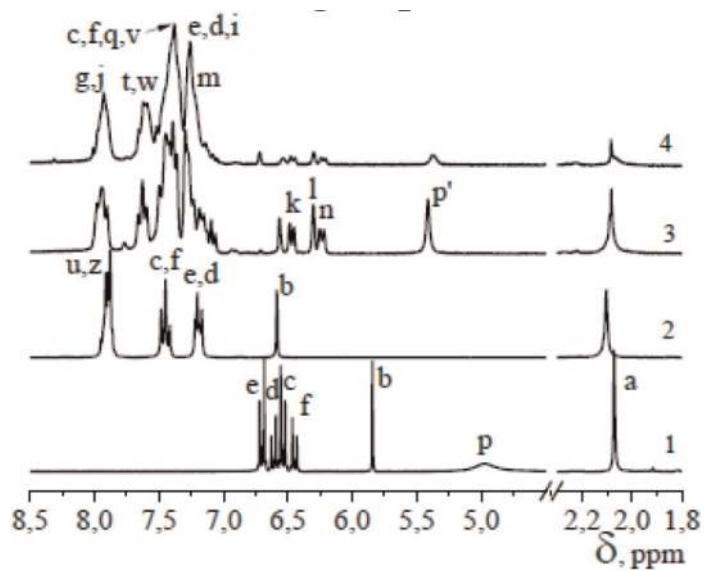


Figure 19.
NMR ^1H spectra of TAPT (1) and TAPT-PA (2), SOI prepared at different 3-APPA/TAPT mole ratios: 10/1 (3) and 40/1 (4).

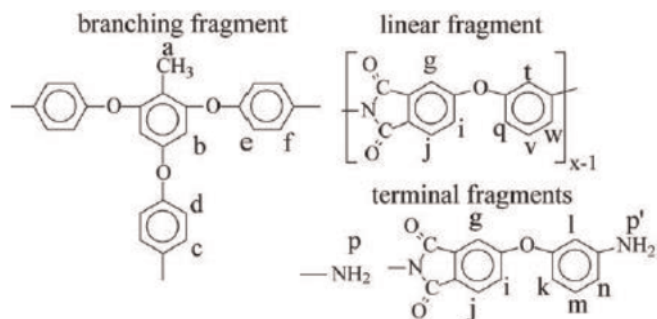


Figure 20.
Assignment of signals in NMR ^1H spectrum to corresponding hydrogen atoms in branching, linear and terminal.

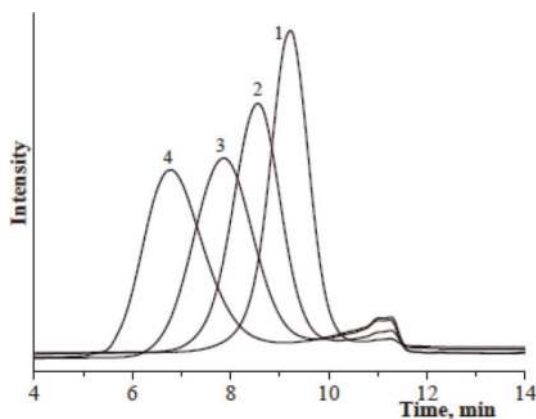


Figure 21. GPC chromatogram of SOI prepared at different APPA/TAPT mole ratios: 10/1 (1), 20/1 (2), 40/1 (3), and 100/1 (4).

Sample APPA/TAPT	M_w	M_n	M_w/M_n	M_w/M_n (without low MW fraction)
SOI 10	13,100	11,600	1.13	1.08
SOI 20	19,800	15,200	1.3	1.08
SOI 40	29,200	16,860	1.73	1.16
SOI 100	53,350	20,700	2.57	1.17
Poly APPA	24,400	9000	2.71	—

Table 7. Molecular weight characteristics of the oligoimides (GPC).

All SOI samples obtained are soluble in chloroform. For samples SOI40 and SOI 100, mechanically strong self-supporting films were obtained by casting from a solution in chloroform. According to DSC, increasing the APPA/TAPT ratio leads to an increase in the glass transition temperature.

In **Figure 21**, the GPC chromatograms of SOI samples are given. With an increase in the total ratio of 3-APPA/TAPT, the main peak on the GPC chromatogram shifts toward high molecular weights accomplished by small broadening of the peaks. All SOI samples have narrow MWD with $M_w/M_n = 1.1$ – 1.2 (**Table 7**), in which values are much less than the corresponding values for PI obtained by APPA auto-polycondensation in molten BA ($M_w/M_n \sim 3$) in the absence of additives. Small polydispersity is very unusual for polycondensation processes. It indicates that there is a selective growth of arms on the initiator molecules, similar to the process of “chain polycondensation” [30].

There is a small peak at low molecular weights in all chromatograms (**Figure 21**). With increasing duration of synthesis, this peak does not change its position. Therefore, we refer it to low molecular cyclic oligomers. The M_w/M_n values calculated without this peak (**Table 7**, columns 5) do not differ much, in all cases $M_w/M_n < 2$. Formation of small quantity of cyclic oligomer can be the evidence of the low-rate by-reaction of AB auto-polycondensation to form linear oligomer with two complementary end groups A and B which can react to give cyclic oligomer.

The effective reactivity of AB in auto-polycondensation and in the reaction with terminal amino group of the growing star is thought to hardly differ from each other. The predominance of selective arm growth and narrow PDI is mainly due to the concentration of terminal arm’s amino groups that is always greater than the current concentration of AB monomer in reaction system.

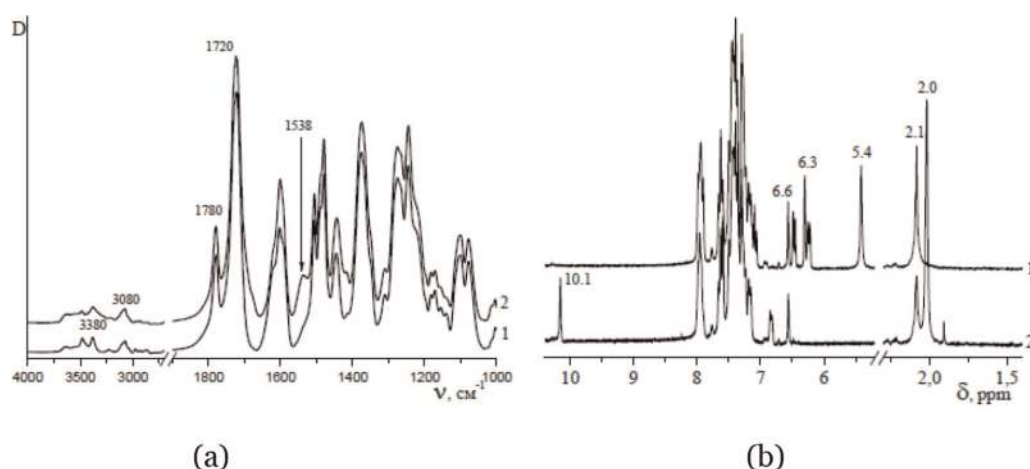


Figure 22. IR spectra (a) and NMR ^1H spectra (b) of SOI 10 (1) and SOI-ac10 (2).

Thus, it is shown that star-shaped oligo- and polyimides with narrow MWD ($M_w/M_n = 1.1\text{--}1.2$) can be synthesized by polycondensation under these conditions.

To confirm the presence of reactive amino groups in SOI molecule, the following experiments were performed. In **Figure 22a**, the IR spectrum is shown of acetyl derivative SOI-ac10 obtained by the treatment of SOI 10 with acetic anhydride. The reaction of SOI with acetic anhydride leads to the disappearance absorption band of the amino group at 3480 cm^{-1} and the appearance of a new band at 1538 cm^{-1} (amide II). In the NMR ^1H spectrum of the SOI-ac10 (**Figure 22b**), the signals at 5.4 ppm (NH₂) and 6.3–6.4 ppm (aromatic protons of terminal moiety) disappear, and new signals appear at 10.1 ppm (—NH—C=O) and 2.0 ppm ($\text{CH}_3\text{—C=O}$), in full correspondence with our expectations.

Presently, two novel tetrafunctional amines and corresponding tetra-arm star-shaped oligomers with $M_w/M_n < 1.6$ were also synthesized via B₄ + AB scheme, where AB is 2-APPA and B₄ is the product of direct condensation of di-N-BOC-protected 3,5-diaminobenzoic acid with aromatic diamines (ODA, AFL) [34] in the presence of triphenyl phosphate-pyridine.

7. Conclusions

1. The one-pot high-temperature catalytic polycondensation of diamines and tetracarboxylic acids dianhydrides in molten benzoic acid at $140\text{--}160^\circ\text{C}$ is a new effective, technologically simple, and ecologically friendly method for obtaining polyimides and copolyimides of different chemical structures and topologies including linear polyimides from low reactive monomers, polyimides based on AB monomers, random and multiblock copolyimides, hyperbranched polyimides, star-shaped oligomers with narrow MMD and controlled arm length, etc.
2. Kinetics and mechanism of this method were investigated in detail. Due to catalysis of the first stage of the process—transient polyamic acid formation, combined with its low equilibrium constant—this stage is kinetically insignificant, and imidization becomes the limiting reaction.
3. Imidization reaction at the conditions of polyimide synthesis at $140\text{--}160^\circ\text{C}$ in molten benzoic acid in open system with slow inert gas flow behaves like

nonreversible reaction. Elimination of both reversible stages in polyimide synthesis makes it possible to control chain microstructure of copolyimides by means of varying intermonomer loading.

4. Mathematical modeling of copolyimide chain microstructure formation in molten BA has been developed. Results of prediction of chain microstructure on the basis of independent kinetic data are in good consistence with experimental values obtained from NMR ^{13}C data of copolyimides.

Acknowledgements


The work is supported by the Russian Foundation of Basic Research, Grant #19-03-00820, and the Ministry of High Education and Science of Russian Federation.

Author details

Kuznetsov Alexander Alexeevich* and Tsegelskaya Anna Yurievna
Enikolopov Institute of Synthetic Polymer Materials RAS, Moscow,
Russian Federation

*Address all correspondence to: kuznets24@yandex.ru

IntechOpen

© 2019 The Author(s). Licensee IntechOpen. This chapter is distributed under the terms of the Creative Commons Attribution License (<http://creativecommons.org/licenses/by/3.0>), which permits unrestricted use, distribution, and reproduction in any medium, provided the original work is properly cited. 

References

- [1] Ghosh M, Mittal K, editors. *Polyimides: Fundamentals and Applications*. New York: Marcel Dekker; 1996. p. 891
- [2] Bessonov M, Koton M, Kudryavtsev V, Layus L. *Polyimides—Thermally Stable Polymers*. New York: Consultant Bureau; 1987. p. 318
- [3] Sroog C. Polyimides. *Progress in Polymer Science*. 1991;**16**:561-694. DOI: 10.1016/0079-6700(91)90010-I
- [4] Ardashnikov A, Kardash I, Pravednikov A. The equilibrium character of the reaction of aromatic anhydrides with aromatic amines and its role during the synthesis of polyimides. *Polymer Science U.S.S.R.* 1971;**8**:1863-1869. DOI: 10.1016/0032-3950(71)90411-4
- [5] Kardash I, Ardashnikov A, Lavrov S, Pravednikov A, et al. The role of equilibrium state of the reaction of formation of polyamido acids in the process of their thermal cyclization in solution. *Russian Chemical Bulletin*. 1979;**28**:1983. DOI: 10.1007/BF00952499
- [6] Korshak V, Vinogradova S, Vygodskii Ya, Pavlova S, Boiko L. Thermally stable soluble polyimides. *Russian Chemical Bulletin*. 1967;**16**: 2172-2178. DOI: 10.1007/BF00913301
- [7] Vinogradova S, Vygodskii Ya, Korshak V. Some features of the synthesis of polyimides by single-stage high-temperature polycondensation. *Polymer Science U.S.S.R.* 1970;**12**: 2254-2262. DOI: 10.1007/BF01106305
- [8] Vinogradova S, Vasnev V, Vygodskii Ya. Cardo polyheteroarylenes. Synthesis, properties, and characteristic features. *Russian Chemical Reviews*. 1996;**65**:249-277. DOI: 10.1070/RC1996v065n03ABEH000209
- [9] Lozinskaya E, Shaplov A, Vygodskii Ya. Direct polycondensation in ionic liquids. *European Polymer Journal*. 2004;**40**:2065-2075. DOI: 10.1016/j.eurpolymj.2004.05.010
- [10] Said-Galiyev E, Vygodskii Ya, Nikitin L, Vinokur R, Khokholov A, Pototskaya I, et al. Synthesis of polyimides in supercritical carbon dioxide. *Polymer Science, Russia*. 2004;**46**:634-638. DOI: 10.1016/S0896-8446(03)00146-3
- [11] RF Patent No. 1809612. 1996
- [12] Kuznetsov A, Tsegelskaya A, Belov M, Berendyaev V, Lavrov S, Semenova G, et al. Acid-catalyzed reactions in polyimide synthesis. *Macromolecular Symposia*. 1998;**128**:203-219. DOI: 10.1002/masy.201600202
- [13] Kuznetsov A. One-pot polyimide synthesis in carboxylic acid medium. *High Performance Polymers*. 2000;**12**:445-460. DOI: 10.1134/S0965545X0711003X
- [14] Vygodskii Ya, Spirina T, Nechayev P, Chudina L, Zaikov G, Korshak V, Vinogradova S. The study of the kinetics of formation of poly(amido)acids for carding. *Polymer Science U.S.S.R.* 1977;**19**:1738-1745. DOI: 10.1016/0032-3950(77)90186-1
- [15] Kuznetsov A, Semenova G, Tsegel'skaya A, Yablokova M, Krasovskii V. Interaction of diamines with benzoic acid without a solvent: IR study and phase diagram analysis. *Russian Journal of Applied Chemistry*. 2008;**81**:78-81. DOI: 10.1134/S1070427208010187
- [16] Kuznetsov A, Tsegelskaya A, Buzin P, Yablokova M, Semenova G. High temperature polyimide synthesis in "active" medium: Reactivity leveling of

the high and the low basic diamines. *High Performance Polymers*. 2007;**19**: 711-721. DOI: 10.1177/0954008307081214

[17] Kuznetsov A, Tsegelskaya A, Buzin P. One-pot high-temperature synthesis of polyimides in molten benzoic acid: Kinetics of reactions modeling stages of polycondensation and cyclization. *Polymer Science, Series A*. 2007;**49**: 1157-1164. DOI: 10.1134/S0965545X0711003X

[18] Vasnev V, Kuchanov S. Non-equilibrium copolycondensation in homogeneous systems. *Russian Chemical Reviews*. 1973;**42**: 1020-1033. DOI: 10.1070/RC1973v042n12ABEH002782

[19] Kuznetsov A, Tsegelskaya A, Perov N. ¹³C-NMR analysis of chain microstructure of copolyimides on the basis of 2,2-bis[(3,4-dicarboxyphenoxy)phenyl]propane dianhydride synthesized in molten benzoic acid. *High Performance Polymers*. 2012;**24**: 58-63. DOI: 10.1177/0954008311429501

[20] Batuashvili M, Tsegelskaya A, Perov N, Semenova G, Abramov I, Kuznetsov A. Chain microstructure of soluble copolyimides containing moieties of aliphatic and aromatic diamines and aromatic dianhydrides prepared in molten benzoic acid. *High Performance Polymers*. 2014;**26**:470-476. DOI: 10.1177/0954008313518950

[21] Yamadera R, Murano M. The determination of randomness in copolyesters by high resolution nuclear magnetic resonance. *Journal of Polymer Science Part A: Polymer Chemistry*. 1967;**5**:2259-2268. DOI: 10.1002/pol.1967.150050905

[22] Vygodskii Ya, Vinogradova S, Nagiev Z, et al. A study of copolyimide synthesis, structure and properties. *Acta*

Polymerica. 1982;**33**:131. DOI: 10.1002/actp.1982.010330206

[23] Batuashvili M, Tsegelskaya A, Perov N, Semenova G, Orlinson B, Kuznetsov A. Formation of the chain microstructure in the synthesis of adamantane containing copolyimides in molten benzoic acid. *Russian Chemical Bulletin*. 2015;**64**:930-935. DOI: 10.1007/s11172-015-0957-8

[24] Batuashvili M, Kaminskii V, Tsegelskaya A, Kuznetsov A. Formation of the chain microstructure in copolyimide synthesis by high-temperature polycondensation in molten benzoic acid. *Russian Chemical Bulletin*. 2014;**63**:2711-2718. DOI: 10.1007/s11172-014-0804-3

[25] Kuznetsov A, Batuashvili M, Kaminskii V. Modeling of copolyimide chain microstructure formation in a course of the one-pot copolycondensation in molten benzoic acid. *High Performance Polymers*. 2017;**29**:716-723. DOI: 10.1177/0954008317702953

[26] Kuznetsov A, Akimenko S, Tsegelskaya A, Perov N, Semenova G, Shakhnes A, et al. Synthesis of branched polyimides based on 9,9-bis(4-aminophenyl)fluorene and an oligomeric trianhydride, a 1,3,5-triaminotoluene derivative. *Polymer Science, Series B*. 2014;**56**:41-48. DOI: 10.1134/S1560090414010060

[27] Chukova S, Shakhnes A, Perov N, Krasovskii V, Shevelev S, Kuznetsov A. 2,4,6-Tris(4-aminophenoxy)toluene and hyperbranched polyimide derived from it. *Russian Chemical Bulletin*. 2015;**64**:473-474. DOI: 10.1007/s11172-015-0890-x

[28] Tsegelskaya A, Dutov M, Serushkina O, Semenova G, Kuznetsov A. The one-stage synthesis of hyperbranched polyimides by (A₂+B₄) scheme in catalytic solvent.

Macromolecular Symposia. 2017;**375**:
1600202. DOI: 10.1002/masy.2016
00202

[29] Buzin P, Yablokova M, Kuznetsov
A, Smirnov A, Abramov I. New AB
polyetherimides obtained by direct
polycyclocondensation of
aminophenoxy phthalic acids. High
Performance Polymers. 2004;**16**:
505-514. DOI: 10.1177/09540083040
39991

[30] Gao H. Development of star
polymers as unimolecular containers for
nanomaterials. Macromolecular Rapid
Communications. 2012;**33**:722-734. DOI:
10.1002/marc.201200005

[31] Sugi R, Hitaka Y, Yokoyama A,
Yokozawa T. Well-defined star-shaped
aromatic polyamides from chain-growth
polymerization of phenyl 4-
(alkylamino)benzoate with
multifunctional initiators.
Macromolecules. 2005;**38**:5526-5531.
DOI: 10.1021/ma0473420

[32] Kuznetsov A, Soldatova A,
Tokmashev R, Tsegelskaya A, Semenova
G, Shakhnes A, et al. Synthesis of
reactive three-arm star-shaped
oligoimides with narrow molecular
weight distribution. Journal of Polymer
Science, Part A: Polymer Chemistry.
2018;**56**:2004-2009. DOI: 10.1002/
pola.29088

[33] Tsegelskaya A, Soldatova A,
Semenova G, Dutov M, Abramov I,
Kuznetsov A. One-stage high
temperature catalytic synthesis of star-
shaped oligoimides by (B₄+AB) scheme.
Polymer Science, Series B. 2019;**61**:
148-154. DOI: 10.1007/s11172-018-
2345-7

[34] Soldatova A, Tsegelskaya A,
Semenova G, Abramov I, Kuznetsov A.
Synthesis of tetrafunctional aromatic
amines and star-shaped oligoimides
using the B₄+AB scheme. Russian
Chemical Bulletin. 2018;**67**:2152-2154.
DOI: 10.1007/s11172-0182345-7